

Quantitative analysis of the expression of ACAT¹ genes in human tissues by real-time PCR²

Jeffery L. Smith,^{3,*†} Kavitha Rangaraj,* Robert Simpson,* Donald J. Maclean,*
Les K. Nathanson,[†] Katherine A. Stuart,[§] Shaun P. Scott,** Grant A. Ramm,** and John de Jersey*

Department of Biochemistry and Molecular Biology* and Department of Surgery,[†] University of Queensland, Brisbane 4072, Australia; Department of Gastroenterology and Hepatology,[§] Princess Alexandra Hospital, Brisbane 4102, Australia; and The Queensland Institute of Medical Research,** Brisbane 4006, Australia

Abstract ACAT (also called sterol *o*-acyltransferase) catalyzes the esterification of cholesterol by reaction with long-chain acyl-CoA derivatives and plays a pivotal role in the regulation of cholesterol homeostasis. Although two human ACAT genes termed *ACAT-1* and *ACAT-2* have been reported, prior research on differential tissue expression is qualitative and incomplete. We have developed a quantitative multiplex assay for each ACAT isoform after RT treatment of total RNA using TaqMan real-time quantitative PCR normalized to β -actin in the same reaction tube. This enabled us to calculate the relative abundance of transcripts in several human tissues as an *ACAT-2/ACAT-1* ratio. In liver ($n = 17$), *ACAT-1* transcripts were on average 9-fold (range, 1.7- to 167-fold) more abundant than *ACAT-2*, whereas in duodenal samples ($n = 10$), *ACAT-2* transcripts were on average 3-fold (range, 0.39- to 12.2-fold) more abundant than *ACAT-1*. *ACAT-2* was detected for the first time in peripheral blood mononuclear cells. Interesting differences in *ACAT-2* mRNA expression were evident in subgroup analysis of samples from different sources. These results demonstrate quantitatively that *ACAT-1* transcripts predominate in human liver and *ACAT-2* transcripts predominate in human duodenum and support the notion that *ACAT-2* has an important regulatory role in liver and intestine.—Smith, J. L., K. Rangaraj, R. Simpson, D. J. Maclean, L. K. Nathanson, K. A. Stuart, S. P. Scott, G. A. Ramm, and J. de Jersey. **Quantitative analysis of the expression of ACAT genes in human tissues by real-time PCR.** *J. Lipid Res.* 2004. 45: 686–696.

Supplementary key words acyl-coenzyme A:cholesterol acyltransferase • atherosclerosis • cholesterol metabolism • duodenum • gallstones • intestine • liver • sterol *o*-acyltransferase

ACAT [also called sterol *o*-acyltransferase (SOAT); EC 2.3.1.26] is localized in the endoplasmic reticulum of cells and catalyzes the esterification of cholesterol by reaction with long-chain fatty acyl-CoA derivatives. Since its initial discovery in rat liver (1, 2), ACAT activity has been de-

tected in a diverse range of tissues and cell types (3) and is known to play an important role in cell biology and in the pathogenesis of important lipid-related diseases such as atherosclerosis (3) and cholesterol gallstones (4). For example, ACAT has been shown to play a pivotal functional role in the intestinal absorption of cholesterol, the hepatic secretion of VLDL, the biosynthesis of steroid hormones, the production of cholesteryl esters in macrophages (foam cells) in atheroma, and the secretion of biliary cholesterol. From a biochemical and physiological perspective, ACAT is one of the central enzymes regulating plasma and biliary cholesterol concentrations. An excess of plasma cholesterol can lead to atherosclerosis, and an increased secretion of cholesterol in bile can predispose individuals to cholesterol gallstones. Not surprisingly, ACAT has been the focus of considerable research during the past decade because of its obvious pharmacological relevance.

Two ACAT genes are known in humans. The first ACAT gene, cloned by Chang and colleagues (5) in 1993, is now termed *ACAT-1*. The second, *ACAT-2*, was cloned in 1998 (6–8). The two genes have 47% overall nucleotide identity (5, 8) and encode specific ACAT proteins that have 43% amino acid sequence identity and 63% similarity. These landmark studies (5–8) using gel-based detection of ACAT mRNA (RT-PCR and Northern blot analysis) provide evidence that *ACAT-2* is expressed primarily in liver and in-

Abbreviations: PBMC, peripheral blood mononuclear cells; RT-PCR, RT treatment of RNA followed by quantitative real-time PCR.

¹ The official name for the enzyme known widely as acyl-coenzyme A:cholesterol acyltransferase (ACAT) is sterol *o*-acyltransferase (SOAT) (<http://www.gene.ucl.ac.uk/cgi-bin/nomenclature/searchgenes.pl>). However, as ACAT is an accepted abbreviation of this enzyme for this journal and remains an accepted alias of SOAT (<http://www.gene.ucl.ac.uk/cgi-bin/nomenclature/searchgenes.pl>), we have referred to it as ACAT throughout this article.

² A portion of this work was presented in abstract form to the 73rd European Atherosclerosis Society Meeting, Salzburg, Austria, July 7–10, 2002.

³ To whom correspondence should be addressed.
e-mail: jefferysmith@optusnet.com.au

Manuscript received 29 August 2003 and in revised form 3 December 2003.

Published, JLR Papers in Press, January 16, 2004.

DOI 10.1194/jlr.M300365JLR200

testine, whereas *ACAT-1* is expressed in a wide variety of tissue types. Human *ACAT-2* mRNA has been detected by RT-PCR in a number of cell types, including hepatocyte (HepG2 cells) (6, 8) and intestinal epithelial cells (Caco2 cells) (8). However, detectable levels of *ACAT-2* were not observed in human fibroblasts (6), undifferentiated THP1 cells (monocytes) (8), or differentiated THP1 cells (macrophages) (8). In contrast, *ACAT-1* mRNA has been detected by RT-PCR in all of these cell types (6, 8). Working with cells isolated from monkey liver, Rudel and colleagues (7) estimated by Northern blot analysis that the *ACAT-1* mRNA level in hepatocytes was approximately half that in Kupffer cells, whereas the *ACAT-2* mRNA level in hepatocytes was approximately six times that found in Kupffer cells. They concluded that both *ACAT-1* and *ACAT-2* are present in hepatocytes, whereas Kupffer cells contain predominantly, if not solely, *ACAT-1*. Although important tissue expression information was provided by these initial studies (5–8), the precise relative intratissue and intertissue/cellular expression levels of the two ACAT isoforms, especially in human tissues, are uncertain because of limitations in the methodologies used.

Our understanding of the physiological role of the two ACAT isoforms is incomplete. One school of thought states that the ACAT-1 protein has a major catalytic role in human liver but not intestine (9) and that ACAT-2 is only important in fetal, not adult, liver and intestine (10). Others propose that ACAT-1 is much less physiologically important in liver because it is predominantly expressed in Kupffer cells, whereas ACAT-2 is more important in both liver and intestine because it is expressed solely in hepatocytes and in the apical third of intestinal mucosal cells of nonhuman primates (11). The latter study is consistent with the finding that total hepatic ACAT enzyme activity and hepatic cholesteryl ester levels are normal in *ACAT-1* gene knockout mice (12). Furthermore, membrane topology studies indicated that the catalytic serine of each isoform is located on opposite sides of the endoplasmic reticulum membrane, further supporting disparate physiological functions for each isoform (13). As a working hypothesis, it has been proposed that ACAT-1 is constitutively expressed and likely functions to maintain the intracellular balance of free and esterified cholesterol, whereas ACAT-2 is associated with intestinal cholesterol absorption and hepatocyte-specific functions such as lipoprotein particle assembly and the production of bile (6–15).

In the absence of reliable quantitative assays for activity, protein, and mRNA levels for *ACAT-1* and *ACAT-2*, the physiological importance of the two ACAT genes and their products cannot be defined with any certainty. This lack of quantitative data makes it difficult to design specific ACAT modulators to influence hepatic VLDL and biliary cholesterol secretion, cholesterol absorption from the diet, and cholesteryl ester formation in atheromatous plaque. The aims of the present study were 2-fold: *a*) to develop improved procedures to quantify the abundance of *ACAT-1* and *ACAT-2* transcripts in human tissues; and *b*) to apply these procedures to the analysis of various human tissues, particularly liver and duodenum, from a variety of

individuals. Real-time RT treatment of RNA followed by quantitative real-time PCR (RT-qPCR) technology was chosen because *i*) the relative abundance of each transcript isoform can be determined using specific primers and hybridization probes; *ii*) it is highly sensitive and quantitative compared with alternative technologies; *iii*) it allows fast analysis and throughput with excellent quality control; and *iv*) the relative abundance of transcripts can be compared for different samples assayed on different occasions (16).

MATERIALS AND METHODS

Clinical samples

Clinical material was obtained from a variety of sources (Table 1) with appropriate consent. The Royal Brisbane, Mater Misericordiae, Greenslopes Private, and/or Princess Alexandra Hospital ethics committees approved all procedures and protocols used. Most liver samples were obtained from organ donors after obtaining consent for the use of tissue for scientific purposes from the next of kin. A sample of spleen was also obtained from one of the organ donors. Some liver samples were also obtained from patients undergoing cholecystectomy for gallstones and liver biopsy. Extensive studies by our group have demonstrated that total ACAT enzyme activity is clinically relevant and comparable in liver samples from these sources (4, 17, 18). Furthermore, useful data on the abundance of transcripts unrelated to ACAT have been obtained from some of these same samples (19). Duodenal biopsies were obtained from patients having gastroscopy for clinically indicated reasons, such as investigation for abdominal pain, iron deficiency, weight loss, anemia, and reflux. Biopsies were performed by a single gastroenterologist and were taken from the second part of the duodenum and contained predominantly intestinal mucosal cells (mostly enterocytes with some goblet, Paneth, and endocrine cells). Each biopsy is also likely to have contained small numbers (<5%) of fibroblasts, lymphoblasts, macrophages, and connective tissue and muscle cells. Normal kidney samples adjacent to cancerous tissue were collected at the time of nephrectomy from patients with renal cell carcinoma. As soon as tissue samples were available, they were plunged into liquid nitrogen and stored at -80°C until processed. Peripheral blood mononuclear cells (PBMC) were isolated immediately from freshly collected whole blood taken from healthy volunteers and patients with confirmed cholesterol gallstones (after cholecystectomy) using Ficoll gradient centrifugation (Ficoll Hypaque; Pharmacia). The clinical characteristics of the subjects and patients from whom samples were collected are shown in Table 1.

Extraction of total RNA and production of cDNA

RNA samples were isolated from clinical samples using TRI Reagent (Molecular Research Centre, Inc.) or Trizol (Life Technologies) using protocols recommended by the manufacturers. The amount of tissue used for RNA extraction was 50–100 mg for liver, spleen, and duodenal biopsies and 10 ml of whole blood for PBMC. cDNA was generated from 0.5–2 μg samples of total RNA at 42°C for 50 min (reaction volume, 10 μl) using random hexamer primers and reverse transcriptase (Superscript II; Life Technologies) using protocols recommended by the manufacturer.

Primer and TaqMan probe design

To avoid possible signal production from potential contaminating genomic DNA, specific primers for each ACAT gene were

TABLE 1. Clinical characteristics of subjects and patients

Sample Label	Tissue Type	Age	Sex	Subject/Patient Group or Investigation	Warm Ischemia Time
		years			min
1	Liver	24	Male	Liver donor	0
2	Liver	37	Male	Liver donor	0
3	Liver	48	Male	Liver donor	0
4	Liver	48	Female	Liver donor	0
5	Liver	41	Male	Liver donor	0
6	Liver	43	Female	Liver donor	0
7	Liver	38	Male	Liver donor	0
8	Liver	14	Female	Liver donor	0
9	Liver	50	Female	Liver donor (>60% fat)	0
10	Liver	22	Male	Liver donor (visual gallstones)	0
11	Liver	72	Female	Gallstone patient + simvastatin	0
12	Liver	65	Male	Gallstone patient + simvastatin	0
13	Liver	9	Female	Kidney donor	21
14	Liver	61	Female	Kidney donor	24
15	Liver	71	Male	Liver resection	75
16	Liver	55	Female	Liver resection	90
17	Liver	58	Female	Liver resection	120
A	Duodenum	57	Female	Iron deficiency	0
B	Duodenum	63	Female	Iron deficiency	0
C	Duodenum	61	Female	Iron deficiency: insulin-dependent type 2 diabetic with chronic renal failure	0
D	Duodenum	25	Male	Abdominal pain	0
E	Duodenum	39	Male	Abdominal pain	0
F	Duodenum	41	Male	Abdominal pain	0
G	Duodenum	54	Male	Abdominal pain	0
H	Duodenum	48	Male	Weight loss	0
I	Duodenum	32	Male	Reflux	0
J	Duodenum	72	Female	Anemia	0
a	Kidney	N/A	N/A	Renal cell carcinoma	0
b	Kidney	N/A	N/A	Renal cell carcinoma	0
c	Kidney	N/A	N/A	Renal cell carcinoma	0
	Spleen			Organ donor	0
a	PBMC	39	Male	Healthy control	0
b	PBMC	34	Female	Healthy control	0
c	PBMC	31	Female	Healthy control	0
d	PBMC	29	Female	Healthy control	0
e	PBMC	49	Female	Cholesterol gallstones	0
f	PBMC	25	Female	Cholesterol gallstones	0
g	PBMC	24	Female	Cholesterol gallstones	0

Warm ischemia time is lack of blood flow to the tissue at 37°C before sample collection. N/A, not available; PBMC, peripheral blood mononuclear cells.

designed across a common exon-exon splice junction selected as described below from the published full-length cDNA sequences (8, 20). At the time this work was undertaken, the exon-intron boundary junctions were known only for *ACAT-1* (20). Using the published cDNA sequence of *ACAT-2* (8), we found its cognate genomic sequence in the human sequence database, and an alignment identified 15 exons for human *ACAT-2*, subsequently verified by Song et al. (21). In comparison, *ACAT-1* has 16 exons that subtend 15 introns (20). Although the first intron of *ACAT-1* appears to be absent from *ACAT-2*, most of the other intron splice sites for *ACAT-1* and *ACAT-2* are highly conserved (see Results). Exons and introns for *ACAT-1* and their *ACAT-2* homologs are numbered elsewhere in this article according to the *ACAT-1* designations of Li et al. (20). From an alignment of the *ACAT-1* and *ACAT-2* cDNAs, we identified the splice site joining exons 5 and 6 (i.e., the exon 5/6 junction) common to the *ACAT-1* and *ACAT-2* genes as showing suitable sequence divergence and GC content for the design of cDNA-specific PCR primers, including one that spans the splice junction. Forward and reverse primers and TaqMan probes specific for *ACAT-1* and *ACAT-2*, respectively, were designed for the real-time PCR assays using Primer Express software version 5 (Applied Biosystems) as shown below. Arrows (↓) indicate the locations of the splice junctions. *ACAT-1* as-

say (amplicon size 89 nucleotides): forward primer, 5'-CAAG-GCGCTCTCTCTTAGA↓TGAAC-3'; reverse primer, 5'-GATAAA-GAGAATGAGGAGGGCAATAA-3'; probe, 5'-(FAM)-CTTGAAG-TGGACCACATCAGAACAATATATCACATG-(TAMRA)-3'. *ACAT-2* assay (amplicon size 70 nucleotides): forward primer, 5'-GCA-AGTCCCTGCTTGA↓TGAGC-3'; reverse primer, 5'-CCAGCGAT-GAACATGTGGTAGAT-3'; probe, 5'-(FAM)-TGCGGAAATGCT-GCACCTCCAT-(TAMRA)-3'. The TaqMan probes were synthesized with the fluorescent reporter dye FAM (6-carboxy-fluorescein) attached to the 5'-end and the quencher dye TAMRA (6-carboxy-tetramethyl-rhodamine) attached to the 3'-end. All primer sets and TaqMan probes for the ACAT assays and the actin primer/probe set (predeveloped assay reagent for human β -actin labeled at the 5'-end with the reporter dye VICTM) were obtained from Applied Biosystems.

Multiplex RT-qPCR assays with β -actin

The cDNA representing each ACAT isoform was quantitated by PCR using an ABI model 7700 Sequence Detector (Applied Biosystems) with the specific primers and TaqMan probes described above. Reagent concentrations and PCR conditions were optimized to enable assays of *ACAT-1* (FAM-labeled probe) and β -actin (VIC-labeled probe) to be multiplexed in a single reac-

tion tube and assays of *ACAT-2* (FAM-labeled probe) and β -actin (VIC-labeled probe) to be multiplexed in a separate reaction tube. PCR products (25 μ l final volume) contained 0.3 μ M of each *ACAT* primer and 0.2 μ M of their cognate TaqMan probe, 1.25 μ l of the human β -actin primer/probe reagent (Applied Biosystems; catalog number 431088IE), and 12.5 μ l of TaqMan Universal PCR Mix (Applied Biosystems; catalog number 4304437). Reaction mixtures were preincubated for 2 min at 50°C (for hydrolysis of possible contaminating dUTP-containing template produced by previous PCRs in the laboratory). The PCR program was 10 min of Taq Gold activation at 95°C followed by 45 cycles of 15 s at 95°C and 1 min at 60°C (maximum ramping speed between temperatures). Human cDNA equivalent to 20 ng of total RNA from each sample was assayed in each tube. The PCR cycle number at which each assay target reached the threshold detection line was determined (Ct value; see Fig. 1). cDNA samples were assayed on at least two and up to six occasions to check for assay reliability using duplicate assay reactions on each occasion. The Δ Ct for the *ACAT* isoform assayed in each tube was calculated as Δ Ct = [Ct(*ACAT* isoform) - Ct(β -actin)]. Δ Ct values from all assay reactions were pooled to determine the mean Δ Ct value and standard error for each sample. Assuming that transcripts of *ACAT-1* and *ACAT-2* generate equal TaqMan fluorescence signals from each transcript via RT-qPCR, the relative abundance of *ACAT-2* to *ACAT-1* can be calculated by the following equations:

$$\Delta\Delta\text{Ct} = \Delta\text{Ct}(\text{ACAT-2}) - \Delta\text{Ct}(\text{ACAT-1})$$

$$\text{Ratio (ACAT-2)/(ACAT-1)} = 2^{-\Delta\Delta\text{Ct}}$$

For each sample, standard errors (SE) for $\Delta\Delta$ Ct for the difference between the two means were calculated according to Arkin and Colton (22) using the following equation:

$$\text{SE} = [(\sigma_1^2/n_1) + (\sigma_2^2/n_2)]^{1/2}$$

where σ_1 = standard deviation for Δ Ct(*ACAT-1*/actin), σ_2 = standard deviation for Δ Ct(*ACAT-2*/actin), n_1 = number of assays for Δ Ct(*ACAT-1*/actin), and n_2 = number of assays for Δ Ct(*ACAT-2*/actin). Standard errors for ratios of each sample were determined from $(\Delta\text{Ct} + \text{SE})$ and $(\Delta\text{Ct} - \text{SE})$ or $(\Delta\Delta\text{Ct} + \text{SE})$ and $(\Delta\Delta\text{Ct} - \text{SE})$ as detailed in the ABI PRISM 7700 user manual (bulletin 2). To compare sets of different samples, mean values of *ACAT* isoform/ β -actin or *ACAT-2*/*ACAT-1* for each tissue type (see Fig. 4) were calculated directly from the ratio values calculated (via $2^{-\Delta\text{Ct}}$ or $2^{-\Delta\Delta\text{Ct}}$) for each individual sample and are presented \pm SE unless otherwise indicated.

Figure 1 shows typical amplification plots for *ACAT-1*, *ACAT-2*, and β -actin and illustrates how the relative difference in abundance of *ACAT-1* and *ACAT-2* transcripts in a single cDNA sample ($\Delta\Delta$ Ct) was calculated. The amplification plots for β -actin (tubes 1 and 2, Fig. 1A) and *ACAT-1* and *ACAT-2* (tubes 1 and 2, Fig. 1B) have been superimposed to illustrate typical assay data from a single sample. Two independent samples were taken from liver 6 (Table 1), and RNA extracts were prepared and assayed independently by RT-qPCR. Very similar results were obtained, indicating the general reliability of our procedures (data not shown). We have presented the pooled data from liver sample 6.

Validation of the real-time PCR

Short PCR amplicons such as those designed for the *ACAT-1* and *ACAT-2* assays are expected to minimize inaccuracy related to possible differential degradation of RNA samples during extraction and reverse transcription and to enhance the efficiency of the PCR. *ACAT-1* and *ACAT-2* primers and probes were checked for specificity and amplification efficiency by perform-

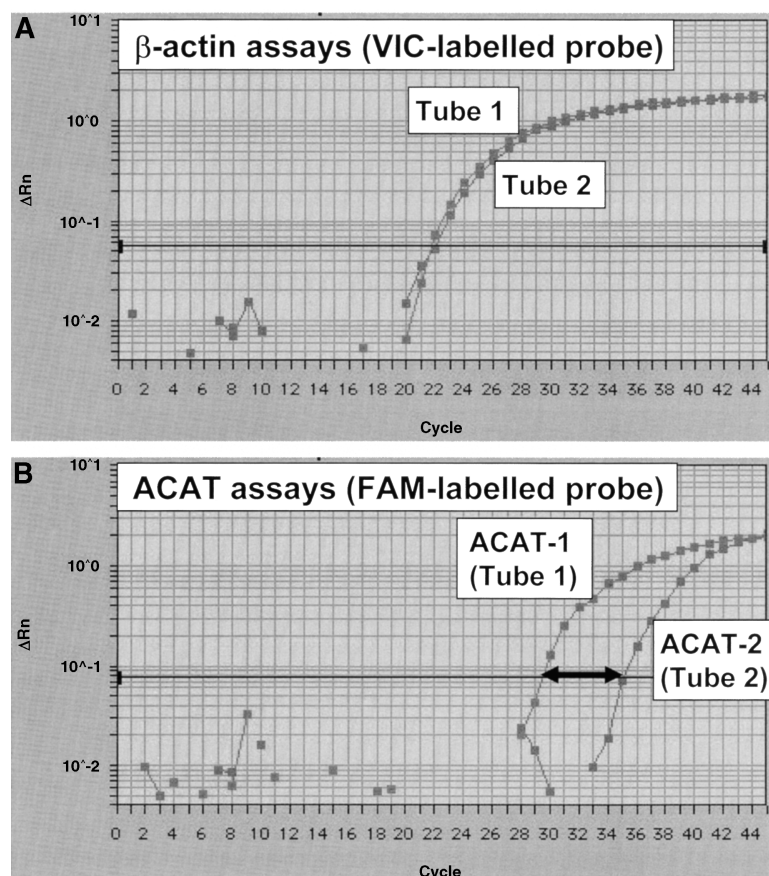


Fig. 1. Typical amplification plots for *ACAT-1*, *ACAT-2*, and β -actin showing how their relative expression levels can be assayed by real-time RT treatment of RNA followed by quantitative real-time PCR (RT-qPCR) using a cDNA template derived from RT treatment of 20 ng of RNA from a single human liver sample. A: Amplification plots for β -actin in the two multiplex tubes used to assay *ACAT-1* (tube 1) and *ACAT-2* (tube 2) are closely superimposed within experimental error. B: Amplification plots for *ACAT-1* and *ACAT-2* in tubes 1 and 2, respectively. The difference between the Ct values for *ACAT-1* and *ACAT-2* (arrow) indicates the $\Delta\Delta$ Ct value as defined in the text. Δ Rn is the relative fluorescence of the reporter dye.

ing real-time PCR assays using clones of each full-length ACAT isoform cDNA as a template. The cloned cDNAs were human *ACAT-1* (pcDNA3; a gift from T-Y. Chang via Sandra Erickson) and human *ACAT-2* (pRS426-GalPro; a gift from Steven Sturley). A 10-fold dilution series for each cloned ACAT cDNA was prepared from 10^7 down to 1 template copy per reaction and assayed by the specific assay for each ACAT isoform. To examine the effect of sample dilution on relative quantitation, a bulk cDNA preparation was made by mixing equal amounts of cDNA derived from liver sample 8 and duodenal sample A, and amounts of the cDNA mixture equivalent to 150, 80, 40, 15, and 5 ng of total RNA were assayed by the multiplex assays.

RESULTS

Development of a multiplex RT-qPCR assay for *ACAT-1* and *ACAT-2*

To assess the expression levels of ACAT transcripts, β -actin was chosen as the reference housekeeping gene because it is conveniently assayed and highly expressed. Furthermore, a predeveloped assay kit for β -actin was commercially available and is used widely in other research (16). To avoid spurious PCR amplification from human genomic DNA, the forward primer for each ACAT isoform was designed to span an exon-exon splice junction common to both *ACAT-1* and *ACAT-2*. As part of the design process, we aligned the cDNA sequences of *ACAT-1* and *ACAT-2* and found that 11 of the 15 splice junctions in *ACAT-1* were identical in *ACAT-2*. The exceptions were the splice sites joining *i)* exons 1/2 (intron 1 was missing from *ACAT-2*); *ii)* exons 2/3 (splice site was 3 bp downstream in *ACAT-2*); *iii)* exons 4/5 (15 nucleotides flanking the *ACAT-1* splice site were deleted from *ACAT-2*, and the splice site for *ACAT-2* was 15 bp upstream from the splice site for *ACAT-1* in the aligned sequence); and *iv)* exons 8/9 (splice site was 10 bp upstream in *ACAT-2*). We chose sequence flanking each side of splice junction 5/6 to design the forward primers for both the *ACAT-1* and *ACAT-2* assays; neither assay produced any amplification signal from genomic DNA template. The manufacturers of the β -actin reference assay kit note that human genomic DNA can give an amplification signal, but in our hands, this was many orders of magnitude less than the signal given by an equivalent amount of cDNA derived by reverse transcription from a total RNA sample (data not shown) and hence insignificant.

Validation of the RT-qPCR assays for *ACAT-1* and *ACAT-2*

To validate the sensitivity and specificity of the primer/probe combinations chosen for each ACAT isoform, we demonstrated that the *ACAT-1* assay detected a cloned *ACAT-1* cDNA template at high sensitivity (e.g., Ct values of 16.5 and 27.2 cycles for 10^7 and 10^4 template copies, respectively) and the *ACAT-2* assay similarly detected a cloned *ACAT-2* cDNA template (e.g., Ct values of 16.3 and 25.8 cycles for 10^7 and 10^4 template copies, respectively). Cross-reactivity was negligible: when using the *ACAT-1* assay, 10^7 copies of the cloned *ACAT-2* cDNA template gave amplification signals equivalent to 10 or fewer copies of

the cloned *ACAT-1* cDNA template, and vice versa for the *ACAT-2* assay. The above data are taken from assays of a dilution series of each cloned ACAT cDNA, which demonstrated that the increase in Ct after each 10-fold dilution approximated the theoretical value of +3.32 cycles expected for maximum (2^n) PCR efficiency. Hence, the primer/probe combinations used for the assay of each ACAT isoform were both highly sensitive and highly specific. These assay protocols were modified for the multiplex assays by adding reagents for the β -actin reference assay at primer-limiting concentrations recommended by the manufacturer to avoid interfering with the amplification kinetics of the test ACAT transcript. The β -actin transcripts were more abundant in all samples tested (i.e., they gave considerably lower Ct values) than the ACAT transcripts (Figs. 1 and 2), a desirable attribute for multiplex assays as it enhances the consistency of ACAT amplification kinetics. The final outcome of the method development was a multiplex assay for each ACAT isoform, allowing *ACAT-1* and β -actin to be multiplexed in a single reaction tube and *ACAT-2* and β -actin to be multiplexed in a separate reaction tube. The results obtained were reliable and reproducible, as indicated by analysis of errors for the ACAT/ β -actin determinations in Figs. 2 and 3 (A and B). Figure 1 shows typical amplification plots for *ACAT-1*, *ACAT-2*, and β -actin to illustrate how the difference in *ACAT-1* and *ACAT-2* transcript abundance in a cDNA sample was determined as $\Delta\Delta Ct$, thus enabling the calculation of *ACAT-2*/*ACAT-1* ratios as described in Materials and Methods.

Because human tissue sample sizes were generally small, it was not feasible to obtain highly purified RNA preparations of accurately known RNA concentration. Hence, we did not attempt to determine "absolute" levels of mRNA transcripts of each ACAT gene (23), and our results are presented as the relative abundance of the various transcript isoforms to each other, assuming equal reverse transcription efficiency from each mRNA molecule. As a further check on the veracity of relative quantitation, we assayed *ACAT-1*, *ACAT-2*, and β -actin in a dilution series of a bulk cDNA preparation derived from mixed liver and intestine RNAs. Pairwise comparisons of data from the different dilutions showed that none of the values of ΔCt for *ACAT-1*/actin, ΔCt for *ACAT-2*/actin, or $\Delta\Delta Ct$ for *ACAT-2*/*ACAT-1* were significantly different from each other (data not shown). Within the experimental errors inherent in the technology, this result indicates that the amplification efficiencies of all three cDNA templates (*ACAT-1*, *ACAT-2*, and β -actin) were approximately the same and supports the data we presented from the dilutions of plasmid-cloned ACAT cDNAs. Agarose gel electrophoresis showed that the PCR-amplified products from the bulk cDNA preparation were of the expected size (data not shown).

Expression of *ACAT-1* and *ACAT-2* in human tissues

ACAT-1 and *ACAT-2* were expressed as low-abundance transcripts relative to β -actin in three different human tissues (liver, duodenum, and kidney; Fig. 2A, B) and PBMC

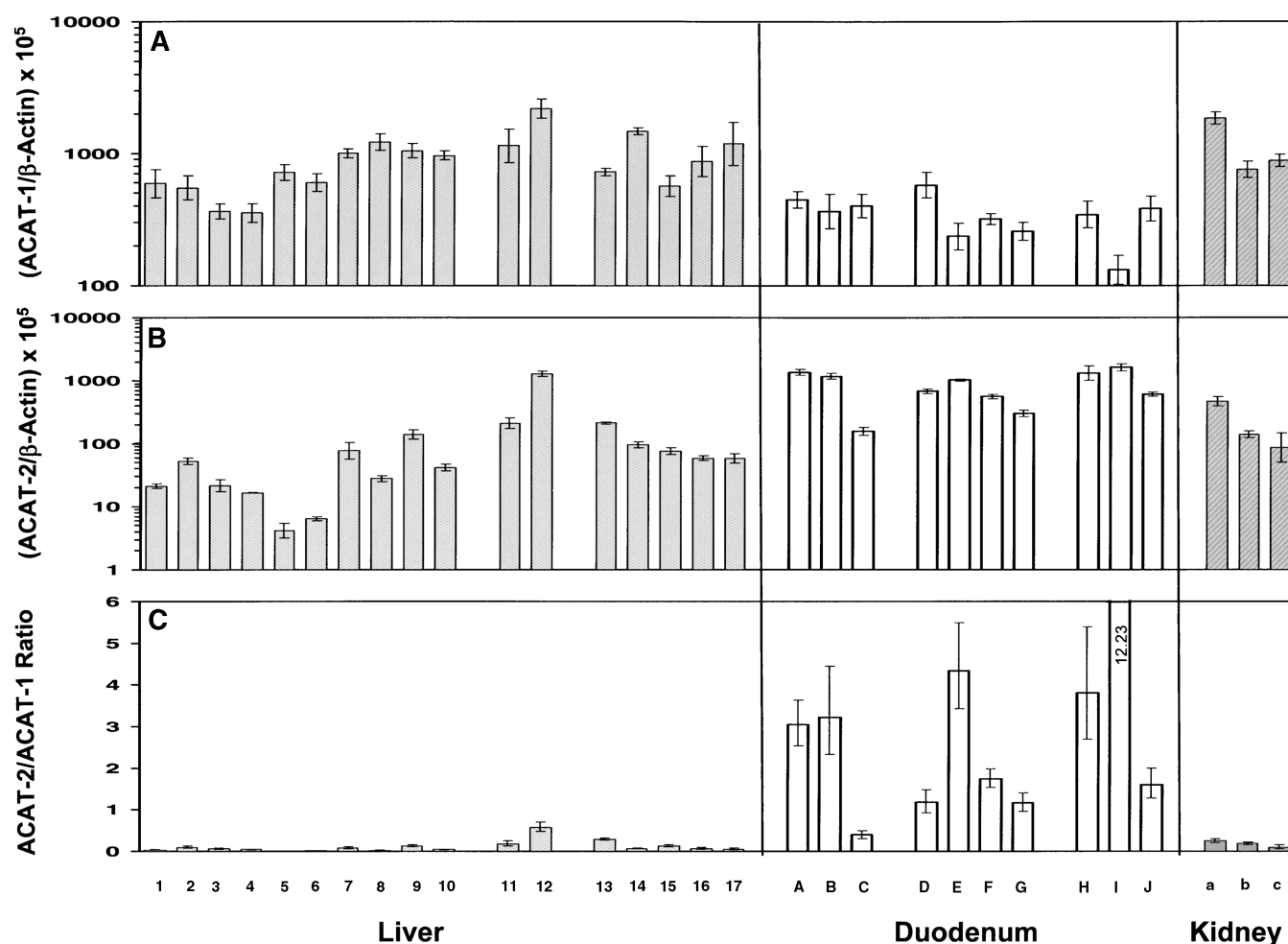


Fig. 2. The relative abundance of *ACAT-1* and *ACAT-2* transcripts in total RNA from different tissue samples was determined by real-time RT-qPCR and expressed relative to β -actin with standard errors for replicate determinations as described in Materials and Methods. Data for liver samples (1–17), duodenum samples (A–J), and kidney samples (a–c) are shown. The subject and patient characteristics from which these samples were taken are given in Materials and Methods and in Table 1. A: *ACAT-1*/ β -actin. B: *ACAT-2*/ β -actin. C: *ACAT-2*/*ACAT-1*. The y axes in A and B are on a log scale to display all data visually, whereas the y axis in C is on a linear scale to highlight the dramatic differences in relative expression between *ACAT-2* and *ACAT-1* in samples from different tissues.

(Fig. 3A, B). Relative to β -actin, expression levels of *ACAT-1* and *ACAT-2* varied considerably in different tissues and are shown on a logarithmic scale in Fig. 2A, B to depict all data visually. Both *ACAT* transcripts were readily detected in all samples, including *ACAT-2* in PBMC, at levels well within the range of sensitivity of the RT-qPCR technology as defined by our dilution series of cloned cDNA templates. Relative expression levels can be estimated by assuming that transcript molecules of each of the three mRNA species assayed generate equal fluorescence signals after reverse transcription and qPCR. The highest expression of the *ACAT-1* transcript was observed in the liver and kidney samples, reaching a maximum abundance of only 1–2% that of the β -actin transcript. The highest expression of *ACAT-2* was observed in duodenum samples, also reaching a maximum abundance of only 1–2% that of the β -actin transcript. As *ACAT-1* expression relative to β -actin was more consistent and at generally higher levels than *ACAT-2* in most of the tissue types examined (see below), we used *ACAT-1* as a reference transcript. Hence, the

expression of transcripts of the two *ACAT* isoforms relative to each other is presented as an *ACAT-2*/*ACAT-1* ratio for each sample (Figs. 2C and 3C). Note that this ratio represents an accurate relative abundance of the two *ACAT* isoforms within each sample because the β -actin housekeeping gene cancels out in the calculation.

The results shown in Figs. 2A and 3A indicate that *ACAT-1* was expressed at appreciable levels (range, 132 to $2,194 \times 10^{-5}$ relative to β -actin) in samples from all tissues and cells examined, albeit clearly lower (relative to β -actin) in duodenum and PBMC than in liver and kidney (Fig. 4). *ACAT-2* expression was even more variable (range, 4 to $1,613 \times 10^{-5}$ relative to β -actin), with transcript levels being relatively high in duodenum and much lower in liver, kidney, and PBMC. Results obtained for a single sample of spleen obtained from an organ donor were similar to those of liver: *ACAT-1*/ β -actin = 547×10^{-5} ; *ACAT-2*/ β -actin = 15.0×10^{-5} . Figures 2C and 3C compare the *ACAT-2*/*ACAT-1* ratio of all samples assayed, using a linear scale in Fig. 2C to demonstrate the dramatic

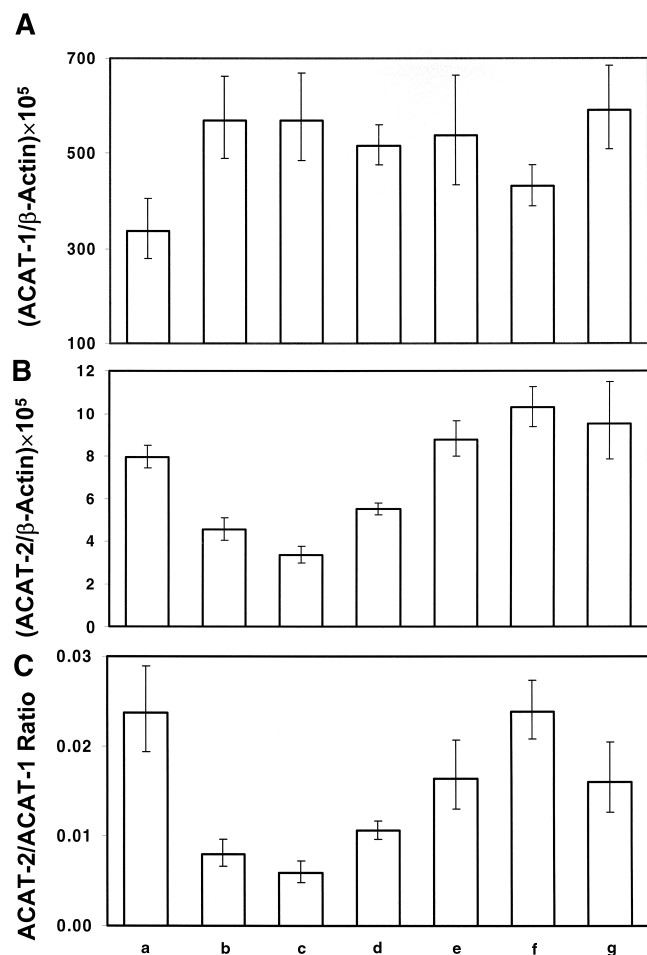


Fig. 3. The relative abundance of *ACAT-1* and *ACAT-2* transcripts in total RNA in peripheral blood mononuclear cells (PBMC) was determined by real-time RT-qPCR and expressed relative to β -actin with standard errors for replicate determinations as described in Materials and Methods. Data for PBMC samples from healthy volunteers (a–d) and from patients with confirmed cholesterol gallstones with a strong family history of gallstones (e–g; see Table 1) are shown. A: *ACAT-1*/ β -actin. B: *ACAT-2*/ β -actin. C: *ACAT-2*/*ACAT-1*.

cally higher expression of *ACAT-2* over *ACAT-1* in duodenal samples compared with the other tissue types assayed.

Figure 4 compares the mean expression values of ratios of *ACAT-1*/ β -actin (A), *ACAT-2*/ β -actin (B), and *ACAT-2*/*ACAT-1* (C), determined from all samples of each tissue type assayed: liver, duodenum, kidney, and PBMC. Tests for significance for pairwise comparisons of each tissue type (except for kidney, which was represented by only three samples) indicated that mean values for all other tissues types presented in Fig. 4A–C were significantly different from each other ($P \leq 0.05$). The most dramatic differences among these tissues are indicated by the *ACAT-2*/*ACAT-1* ratios (Fig. 4C). Hence, the *ACAT-2*/*ACAT-1* ratio was significantly higher in duodenum (mean *ACAT-2*/*ACAT-1* ratio of 3.27) than in PBMC (mean *ACAT-2*/*ACAT-1* ratio of 0.015), liver (mean *ACAT-2*/*ACAT-1* ratio of 0.112), and kidney (mean *ACAT-2*/*ACAT-1* ratio of 0.180). Thus, when expressed as a percentage of total ACAT mRNA, human liver

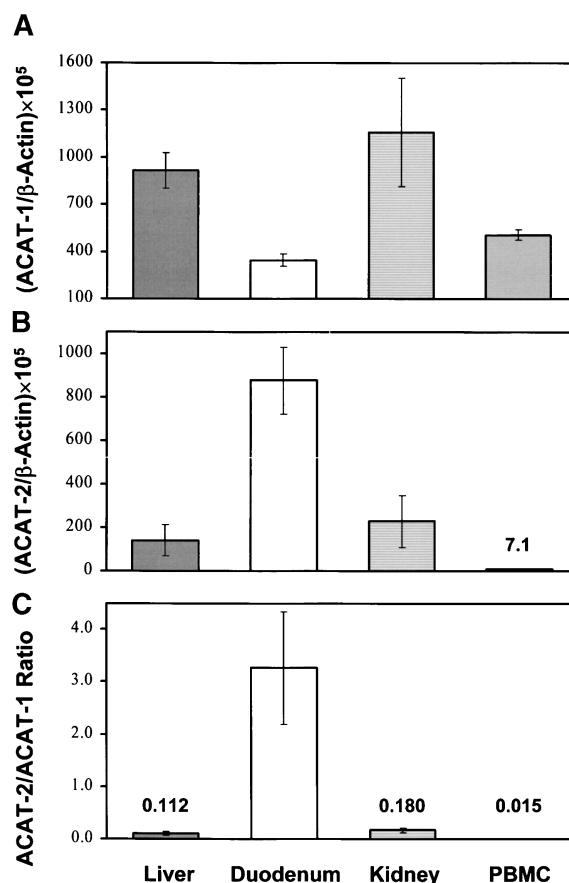


Fig. 4. Mean values (with standard errors) of the abundance of *ACAT-1* and *ACAT-2* transcripts in different tissue types derived from the data for individual samples presented in Figs. 2 and 3. A: *ACAT-1*/ β -actin. B: *ACAT-2*/ β -actin. C: *ACAT-2*/*ACAT-1*. Mean values are presented: liver, $n = 17$; duodenum, $n = 10$; kidney, $n = 3$; PBMC, $n = 7$. Tests for significance (Student's *t*-test for populations with unequal variance) were calculated for pairwise comparisons of each tissue type except for kidney, which was represented by only three samples; mean values for all other tissues were significantly different from each other ($P \leq 0.05$). *ACAT-1*/ β -actin: liver versus duodenum ($P = 0.0001$), liver versus PBMC ($P = 0.0024$), duodenum versus PBMC ($P = 0.007$); *ACAT-2*/ β -actin: liver versus duodenum ($P = 0.0008$), liver versus PBMC ($P = 0.025$), duodenum versus PBMC ($P = 0.0003$); *ACAT-1*/*ACAT-2*: liver versus duodenum ($P = 0.0165$), liver versus PBMC ($P = 0.011$), duodenum versus PBMC ($P = 0.0142$).

constituted 90% *ACAT-1* (range, 77–99% of total ACAT mRNA), i.e., *ACAT-1* was on average nine times more abundant than *ACAT-2*. Conversely, human duodenum constituted 77% *ACAT-2* (range, 28–92% of total ACAT mRNA), i.e., *ACAT-2* was on average 3.3 times more abundant than *ACAT-1*. *ACAT-2* mRNA was more abundant than *ACAT-1* mRNA in all duodenal samples examined except for sample C (Fig. 2B), in which 28% of total ACAT mRNA was *ACAT-2*. *ACAT-2* levels in PBMC were exceedingly low compared with those in the other tissues examined (Fig. 4B).

Subgroup analysis of sample backgrounds

The results obtained for liver, duodenal, and PBMC samples are grouped and numbered in Figs. 2 and 3 ac

cording to patient/subject background (Table 1) to assist in the comparison of expression levels of *ACAT-1* and *ACAT-2* as elaborated below.

Comparison of *ACAT* expression in liver samples. It is possible that sampling methods can alter the levels of transcripts initially present in a living tissue. However, no consistent or significant differences in the expression of either *ACAT* isoform were observed among samples obtained from organ donors (mean \pm SE for samples 1–10, 13, and 14: *ACAT-1*/ β -actin = $801 \pm 99 \times 10^{-5}$; *ACAT-2*/ β -actin = $60 \pm 18 \times 10^{-5}$; and *ACAT-2*/*ACAT-1* = 0.074 ± 0.022) compared with patients undergoing liver resection (samples 15–17: *ACAT-1*/ β -actin = $876 \pm 179 \times 10^{-5}$; *ACAT-2*/ β -actin = $64 \pm 6 \times 10^{-5}$; *ACAT-2*/*ACAT-1* = 0.083 ± 0.026). Warm ischemia time, defined as a period of lack of blood flow to the tissue at 37°C before sample collection (18), varied between 21 and 120 min for samples 13–17 (Table 1). As can be surmised from the data presented in Fig. 2, warm ischemia resulted in increased but not significantly higher levels of *ACAT-1* transcripts (samples 13–17: *ACAT-1*/ β -actin = $967 \pm 164 \times 10^{-5}$) compared with organ donor samples having no warm ischemia time (samples 1–10: *ACAT-1*/ β -actin = $740 \pm 95 \times 10^{-5}$). In contrast, *ACAT-2* transcript levels were significantly higher in warm ischemia samples (samples 13–17: *ACAT-2*/ β -actin = $100 \pm 29 \times 10^{-5}$) compared with control liver samples (samples 1–10: *ACAT-2*/ β -actin = $41 \pm 13 \times 10^{-5}$; $P < 0.05$).

Some liver samples within patient/subject subgroups exhibited *ACAT* expression levels very different from the mean values. Samples 11 and 12 taken from patients with gallstones receiving the drug simvastatin had *ACAT* expression levels, particularly *ACAT-2*, that were markedly higher than other liver samples (*ACAT-1*/ β -actin = $1,146 \times 10^{-5}$ and $2,194 \times 10^{-5}$, *ACAT-2*/ β -actin = 208×10^{-5} and $1,274 \times 10^{-5}$ for samples 11 and 12, respectively; Fig. 2). These differences resulted in higher *ACAT-2*/*ACAT-1* ratios for both samples (sample 11, 0.181; sample 12, 0.580). Other samples showing increased *ACAT-2*/ β -actin levels were sample 13 obtained from a 9 year old kidney donor (213×10^{-5}) and sample 9 taken from a fatty donor liver sample (138×10^{-5}), i.e., samples 13 and 9 were 5.9- and 3.8-fold higher, respectively, than the mean of the other organ donor samples (*ACAT-2*/ β -actin for samples 1–8, 10, and 14 = $36.0 \pm 9.6 \times 10^{-5}$).

Comparison of *ACAT* expression in duodenal samples. Only small numbers of samples represented each subgroup, and apart from one exception, there appeared to be no consistent differences in levels of *ACAT-1* or *ACAT-2* transcripts among the subgroups of patients under investigation for iron deficiency, abdominal pain, weight loss, or anemia. The notable exception was a decreased *ACAT-2* expression level (*ACAT-2*/ β -actin = 157×10^{-5}) in duodenal sample C taken from a 61-year-old female being investigated for iron deficiency. The *ACAT-2*/*ACAT-1* ratio was less than 1.0 for this sample (0.39), indicating that *ACAT-1* was the major isoform, in contrast to all other duodenal samples, which had *ACAT-2* as the major isoform. Patient C was an insulin-dependent type 2 diabetic with chronic renal failure (Table 1).

Comparison of *ACAT* expression in PBMC. Expression levels of *ACAT-1* transcripts in PBMC from healthy volunteers (*ACAT-1*/ β -actin samples a–d: mean \pm SE = $498 \pm 55 \times 10^{-5}$) were comparable to those of patients with confirmed cholesterol gallstones (samples e–g: $520 \pm 47 \times 10^{-5}$; Fig. 3A). In contrast, *ACAT-2*/ β -actin expression levels (Fig. 3B) were 80% greater ($P < 0.05$) in PBMC from cholesterol gallstone patients (samples e–g: $9.5 \pm 0.4 \times 10^{-5}$) compared with healthy controls (samples a–d: $5.3 \pm 1.0 \times 10^{-5}$). When expressed as an *ACAT-2*/*ACAT-1* ratio, the cholesterol gallstone patients had a ratio (0.018 ± 0.003) that was only 50% higher than that of controls (0.012 ± 0.004 ; $0.1 > P > 0.05$) as a result of the low *ACAT-1*/ β -actin value for control sample a.

DISCUSSION

This study describes the development of two RT-qPCR assays to determine the relative abundance of *ACAT-1* and *ACAT-2* mRNA transcripts in human tissue and cell samples. The assay for each *ACAT* isoform was multiplexed with an assay for β -actin in the same reaction tube and used specific TaqMan probes for each target cDNA sequence to generate fluorescence signals. Neither assay generated a signal from genomic DNA, and each assay gave very similar fluorescence signals from equal numbers of copies of a cloned cDNA target. Such multiplex assays have the advantage that knowledge of the exact amount of sample RNA used for each assay (after reverse transcription) is unimportant and results are generated as clearly defined ratios of relative transcript abundance (16, 23). This enabled us to determine the expression levels of both *ACAT-1* and *ACAT-2* relative to β -actin in each sample assayed and hence determine the *ACAT-2*/*ACAT-1* ratio in that tissue. The assays were highly sensitive, specifically detected their intended *ACAT* isoforms, and could be used to compare the relative abundance of transcripts in different samples assayed on different occasions.

Relative expression of *ACAT-1* and *ACAT-2* in various tissues

Expression levels for *ACAT-1* and *ACAT-2* transcripts and values for *ACAT-2*/*ACAT-1* ratios were established for 17 liver, 10 duodenal, 3 kidney, 1 spleen, and 7 PBMC samples (Figs. 2–4). We report that in liver, *ACAT-1* mRNA levels were on average nine times more abundant than *ACAT-2* (*ACAT-2*/*ACAT-1* ratio = 0.112), whereas in duodenal samples, *ACAT-2* transcripts were on average three times as abundant as *ACAT-1* (*ACAT-2*/*ACAT-1* ratio = 3.27). These results demonstrate quantitatively that *ACAT-1* is the predominant transcript isoform in human liver and *ACAT-2* the more abundant isoform in human duodenum, clarifying the somewhat confusing findings of previous gel-based assays using Northern analysis and end point RT-PCR (6–8), as explained in the introduction. Analysis of other tissues showed that in kidney samples, relative levels of *ACAT-1* and *ACAT-2* were in the same range as in liver samples, whereas in PBMC, the *ACAT-2*/*ACAT-1* ra-

tio (0.015) was significantly lower than in all of the other tissues assayed. This is the first report of the presence of *ACAT-2* transcripts in PBMC, and their ready quantitation at low but significant levels opens the way for future analyses of both ACAT transcript isoforms in blood samples.

Previous research has addressed the similarly demanding problem of quantifying levels of the ACAT protein isoforms in human tissues. Expression levels of the ACAT mRNA isoforms found in the present study for liver (mean value of 90% for *ACAT-1*) and intestine (mean value of 77% for *ACAT-2*) are consistent with the specific enzyme activities of the ACAT-1 and ACAT-2 proteins reported by others for human liver and intestine (9). Lee et al. (9) concluded that ACAT-1 represented 90% of total ACAT activity in liver and ACAT-2 represented 81% of total ACAT activity in intestine. Although the mRNA expression levels presented here are consistent with activity levels reported by these workers (9), this does not necessarily imply that transcript levels correlate with their respective ACAT activity levels, as these studies cannot be compared directly. It needs to be highlighted that the methods used by Lee et al. (9) were semiquantitative and based on the immunoprecipitation of solubilized ACAT proteins, methods that are technically very demanding.

Variable ACAT expression in samples representing each tissue/cell type

Having established the veracity of comparing ACAT-2/ACAT-1 ratios in different samples and tissues, we then examined the relative abundance of each isoform in different samples of the same tissue type. For this comparison, we assumed that *β-actin* (as the housekeeping gene) is expressed at similar levels in different samples of the same tissue type (e.g., the 17 liver samples studied here) and calculated standard deviations as a measure of population variability from the mean values. As shown in Fig. 2, *ACAT-1* expression levels (relative to *β-actin*) for liver ranged from 354 to $2,194 \times 10^{-5}$ (mean \pm SD = 916 ± 458 , $n = 17$). For *ACAT-2*, the corresponding range was 4 to $1,274 \times 10^{-5}$ (141 ± 299 , $n = 17$). Thus, ACAT-1/*β-actin* ratios across liver samples were relatively more consistent, varying by 6-fold with the SD $\sim 50\%$ of the mean value, compared with ACAT-2/*β-actin* ratios, which covered a 300-fold range with the SD $\sim 200\%$ of the mean. Duodenum samples showed a similar pattern of variability to liver (Fig. 2), with ACAT-1/*β-actin* covering a 4-fold range: 132 to 576×10^{-5} (346 ± 122 , $n = 10$), and ACAT-2/*β-actin* covering a 10-fold range: 157 to $1,613 \times 10^{-5}$ (878 ± 487 , $n = 10$). Hence, in liver or duodenum sampled from different individuals, *ACAT-2* values were more variable than *ACAT-1* values. Furthermore, little evidence was found for the coordinated regulation of *ACAT-1* and *ACAT-2*, as demonstrated by the variability in ACAT-2/ACAT-1 values among different samples within a tissue type (Fig. 2), e.g., a plot of ACAT-1 versus ACAT-2 expression levels in the same tissue resulted in no association (plot not shown). These data provide evidence that *ACAT-2* is a more likely candidate than *ACAT-1* for regulation in liver and duode-

num and are consistent with the notion that *ACAT-1* is constitutively expressed.

Although ACAT-1 mRNA is known to be expressed in many cell types, including undifferentiated macrophages and fibroblasts (6, 8), *ACAT-2* mRNA has not previously been detected in these cell types (8). Our novel observation that *ACAT-2* mRNA is present in PBMC, albeit at very low levels, indicates that the ACAT-2 enzyme may also have a physiological role in at least some subsets of peripheral cells and tissues represented in PBMC preparations (see below). Total ACAT activity has been determined previously in PBMC and shown to be increased in patients with hyperlipidemia (24). However, unlike ACAT-1, which appears to be involved in cholesteryl ester accumulation in macrophages (25), the role of ACAT-2 in peripheral cells and tissues has yet to be determined.

Absolute expression of ACAT mRNAs in different tissue/cell types?

Although the present work has established reliable quantitative values for the relative abundance of *ACAT-1* and *ACAT-2* transcripts (as ACAT-2/ACAT-1 ratios) in various human RNA samples, it would also be advantageous to compare the absolute levels of each ACAT transcript with total RNA from various cell and tissue types. Although *β-actin* is widely used as a reference housekeeping gene, some studies using RT-qPCR indicate that the absolute abundance of the *β-actin* transcript [e.g., per nanogram of purified poly(A)⁺ RNA after reverse transcription (26)] can vary among different human tissues, and *β-actin* appears to be severalfold more abundant in duodenum than in liver in the study of Medhurst et al. (26). However, there is no easy solution to the problem of finding an absolute reference for expressing transcript abundance; the example cited above (26) presupposes equivalent purification of poly(A)⁺ RNA from total RNA extracted from different tissue types and represents samples pooled from many individuals. Now that real-time PCR analysis is becoming more widely adopted, further critical research is necessary to establish more reliable benchmarks for comparing the abundance of specific ACAT transcripts among tissues and among individuals, e.g., by comparing RT-qPCR assays for various candidate housekeeping genes against total tissue RNA estimated by spectrophotometry and rRNA quantified by RT-qPCR. It is also difficult to determine the efficiency of reverse transcription of various mRNAs when comparing their detection sensitivity, and these issues were not addressed in the research presented here.


Comparison of individuals representing different background groups

When collecting samples for this study, we were able to access samples from a range of individuals exhibiting various disease syndromes or from various physiological or physical backgrounds. Although the numbers of samples in some subgroups are too small to draw any firm conclusions, some differences or trends in ACAT expression levels were observed that might present hypotheses worth ex-

aminating in future research. The most interesting of these observations was the effect of warm ischemia time and expression levels in PBMC from patients with cholesterol gallstones. Warm ischemia time samples showed a trend toward higher ACAT transcript abundance levels, particularly *ACAT-2*, compared with control liver samples, in which warm ischemia time was negligible. This observation contrasts with a previous study by our group (18) showing that total ACAT enzyme activity is markedly decreased by warm ischemia, with a half-life for the loss of activity of 57 min. Until confirmed with a larger number of samples, we recommend that warm ischemia time for all sample types be minimized.

Pilot data from a study of PBMC from patients with confirmed cholesterol gallstones demonstrated that *ACAT-2* mRNA levels were increased by almost 2-fold compared with β -actin levels (Fig. 3B). One might have expected mRNA levels to be decreased given that total hepatic ACAT activity is decreased in patients with cholesterol gallstones (4, 27). The significance of this change is unclear, but it serves as an example that a RT-qPCR method as described here may prove to be a useful noninvasive diagnostic tool, particularly for patients predisposed to cholesterol gallstones, allowing screening of blood samples for defects in lipid metabolism. Further studies on additional gallstone patients and other diseased groups are necessary to assess whether changes in ACAT mRNA isoform levels in PBMC, liver, and/or duodenum correlate with the levels of their cognate protein isoforms and whether such changes can be predictive or causally related to pathogenesis or disease status.

SUMMARY AND CONCLUSIONS

We report the development of two RT-qPCR assays to determine the relative abundance of *ACAT-1* and *ACAT-2* mRNA transcripts in human tissue and cell samples. Our results demonstrate quantitatively that *ACAT-1* transcripts predominate in human liver and *ACAT-2* transcripts predominate in human duodenum and support the notion that *ACAT-2* has an important regulatory role in liver and intestine. To our knowledge, these described assays are the only tools available to quantitate *ACAT-1* and *ACAT-2* mRNA isoforms. These assays, together with methods for ACAT protein isoform analysis such as the immunological methods of Chang and colleagues (9) and Rudel and colleagues (11), provide a range of tools to elucidate the biochemical and physiological roles of ACAT-1 and ACAT-2 in normal and pathophysiological states. However, there is an urgent need for isoform-specific enzyme activity assays suitable for tissue homogenates or subcellular fractions. The identification of specific inhibitors of ACAT isoforms [as described in refs. (6) and (28)] should accelerate progress toward identifying tissue/cell-selective ACAT modulators that better control the regulation of biliary and plasma lipid concentrations that frequently affect lipid-related diseases such as cholesterol gallstones and atherosclerosis. 

For help with the provision and collection of clinical material, the authors thank Leonie Wittenberg, Glenda Balderson, David Nicol, Ian Hardie, and Praga Pillay. The authors also thank Peer Schenk for his assistance with data analysis.

REFERENCES

1. Mukherjee, S., G. Kunitake, and R. B. Alfin-Slater. 1958. The esterification of cholesterol with palmitic acid by rat liver homogenates. *J. Biol. Chem.* **230**: 91–96.
2. Goodman, D. S., D. Deykin, and T. Shiratori. 1964. The formation of cholesterol esters with rat liver enzymes. *J. Biol. Chem.* **239**: 1335–1345.
3. Suckling, K. E., and E. F. Stange. 1985. Role of acyl-CoA:cholesterol acyltransferase in cellular cholesterol metabolism. *J. Lipid Res.* **26**: 647–671.
4. Smith, J. L., I. R. Hardie, S. P. Pillay, and J. de Jersey. 1990. Hepatic acyl-coenzyme A:cholesterol acyltransferase activity is decreased in patients with cholesterol gallstones. *J. Lipid Res.* **31**: 1993–2000.
5. Chang, C. C., H. Y. Huh, K. M. Cadigan, and T. Y. Chang. 1993. Molecular cloning and functional expression of human acyl-coenzyme A:cholesterol acyltransferase cDNA in mutant Chinese hamster ovary cells. *J. Biol. Chem.* **268**: 20747–20755.
6. Cases, S., S. Novak, Y. W. Zheng, H. M. Myers, S. R. Lear, E. Sande, C. B. Welch, A. J. Lusis, T. A. Spencer, B. R. Krause, S. K. Erickson, and R. V. Farese, Jr. 1998. ACAT-2, a second mammalian acyl-CoA:cholesterol acyltransferase. Its cloning, expression, and characterization. *J. Biol. Chem.* **273**: 26755–26764.
7. Anderson, R. A., C. Joyce, M. Davis, J. W. Reagan, M. Clark, G. S. Shelness, and L. L. Rudel. 1998. Identification of a form of acyl-CoA:cholesterol acyltransferase specific to liver and intestine in nonhuman primates. *J. Biol. Chem.* **273**: 26747–26754.
8. Oelkers, P., A. Behari, D. Cromley, J. T. Billheimer, and S. L. Sturley. 1998. Characterization of two human genes encoding acyl coenzyme A:cholesterol acyltransferase-related enzymes. *J. Biol. Chem.* **273**: 26765–26771.
9. Lee, O., C. C. Chang, W. Lee, and T. Y. Chang. 1998. Immunodepletion experiments suggest that acyl-coenzyme A:cholesterol acyltransferase-1 (ACAT-1) protein plays a major catalytic role in adult human liver, adrenal gland, macrophages, and kidney, but not in intestines. *J. Lipid Res.* **39**: 1722–1727.
10. Chang, C. C. Y., N. Sakashita, K. Ornvold, O. Lee, E. T. Chang, R. Dong, S. Lin, C. Y. Lee, S. C. Strom, R. Kashyap, J. J. Fung, R. V. Farese, Jr., J. F. Patoiseau, A. Delhou, and T. Y. Chang. 2000. Immunological quantitation and localization of ACAT-1 and ACAT-2 in human liver and small intestine. *J. Biol. Chem.* **275**: 28083–28092.
11. Lee, R. G., M. C. Willingham, M. A. Davis, K. A. Skinner, and L. L. Rudel. 2000. Differential expression of ACAT1 and ACAT2 among cells within liver, intestine, kidney, and adrenal of nonhuman primates. *J. Lipid Res.* **41**: 1991–2001.
12. Meiner, V. L., S. Cases, H. M. Myers, E. R. Sande, S. Bellosta, M. Schambelan, R. E. Pitas, J. McGuire, J. Herz, and R. V. Farese, Jr. 1996. Disruption of the acyl-CoA:cholesterol acyltransferase gene in mice: evidence suggesting multiple cholesterol esterification enzymes in mammals. *Proc. Natl. Acad. Sci. USA.* **93**: 14041–14046.
13. Joyce, C. W., G. S. Shelness, M. A. Davis, R. G. Lee, K. Skinner, R. A. Anderson, and L. L. Rudel. 2000. ACAT1 and ACAT2 membrane topology segregates a serine residue essential for activity to opposite sides of the endoplasmic reticulum membrane. *Mol. Biol. Cell.* **11**: 3675–3687.
14. Rudel, L. L., and G. S. Shelness. 2000. Cholesterol esters and atherosclerosis—a game of ACAT and mouse. *Nat. Med.* **6**: 1313–1314.
15. Smith, J. L., K. Rangaraj, S. P. Scott, D. J. Maclean, and J. de Jersey. 2002. Role of acyl-coenzyme A:cholesterol acyltransferase (ACAT) in cholesterol gallstone pathogenesis. In Proceedings of the 73rd European Atherosclerosis Society Meeting, Salzburg, Austria. MEDIMOND, Inc., Bologna, Italy. 1–7.
16. Bustin, S. A. 2002. Quantification of mRNA using real-time reverse transcription PCR (RT-PCR): trends and problems. *J. Mol. Endocrinol.* **29**: 23–39.
17. Smith, J. L., J. de Jersey, S. P. Pillay, and I. R. Hardie. 1986. Hepatic acyl-CoA:cholesterol acyltransferase. Development of a standard assay and determination in patients with cholesterol gallstones. *Clin. Chim. Acta.* **158**: 271–282.

18. Smith, J. L., S. P. Pillay, J. de Jersey, and I. R. Hardie. 1989. Effect of ischaemia on the activities of human hepatic acyl-CoA:cholesterol acyltransferase and other microsomal enzymes. *Clin. Chim. Acta.* **84**: 259–268.
19. Bridle, K. R., D. H. G. Crawford, L. M. Fletcher, J. L. Smith, L. W. Powell, and G. A. Ramm. 2003. Evidence for a sub-morphological inflammatory process in the liver in haemochromatosis. *J. Hepatol.* **38**: 425–432.
20. Li, B. L., X. L. Li, Z. J. Duan, O. Lee, S. Lin, Z. M. Ma, C. C. Chang, X. Y. Yang, J. P. Park, T. K. Mohandas, W. Noll, L. Chan, and T. Y. Chang. 1999. Human acyl-CoA:cholesterol acyltransferase-1 (ACAT-1) gene organization and evidence that the 4.3-kilobase ACAT-1 mRNA is produced from two different chromosomes. *J. Biol. Chem.* **274**: 11060–11071.
21. Song, B. L., W. Qj, X. Y. Yang, C. C. Chang, J. Q. Zhu, T. Y. Chang, and B. L. Li. 2001. Organization of human ACAT-2 gene and its cell-type-specific promoter activity. *Biochem. Biophys. Res. Commun.* **282**: 580–588.
22. Arkin, H., and R. R. Colton. 1966. Statistical Methods. 4th edition. Barnes & Noble, New York. 121.
23. Livak, K. J., and T. D. Schmittgen. 2001. Analysis of relative gene expression data using real-time quantitative PCR and $2^{-\Delta\Delta Ct}$ method. *Methods.* **25**: 402–408.
24. Dallongeville, J., J. Davignon, and S. Lussier-Cacan. 1992. ACAT activity in freshly isolated human mononuclear cell homogenates from hyperlipidemic subjects. *Metabolism.* **41**: 154–159.
25. Wang, H., S. J. Germain, P. P. Benfield, and P. J. Gillies. 1996. Gene expression of acyl-coenzyme-A:cholesterol-acyltransferase is upregulated in human monocytes during differentiation and foam cell formation. *Arterioscler. Thromb. Vasc. Biol.* **16**: 809–814.
26. Medhurst, A. D., D. C. Harrison, S. J. Read, C. A. Campbell, M. J. Robbins, and M. N. Pangalos. 2000. The use of TaqMan RT-PCR assays for semiquantitative analysis of gene expression in CNS tissues and disease models. *J. Neurosci. Methods.* **98**: 9–20.
27. Smith, J. L., P. D. Roach, L. N. Wittenberg, M. Riottot, S. P. Pillay, P. J. Nestel, and L. K. Nathanson. 2000. Effects of simvastatin on hepatic cholesterol metabolism, bile lithogenicity and bile acid hydrophobicity in patients with gallstones. *J. Gastroenterol. Hepatol.* **15**: 871–879.
28. Lada, A. T., M. Davis, C. Kent, J. Chapman, H. Tomoda, S. Omura, and L. L. Rudel. 2004. Identification of ACAT1- and ACAT2-specific inhibitors using novel, cell-based fluorescent assay: evidence defining uniqueness for individual ACAT's. *J. Lipid Res.* **45**: 378–386.